THE JOURNAL OF BIOLOGICAL CHEMISTRY
Vol. 279, No. 50, Issue of December 10, pp. 52150–52159, 2004
Printed in U.S.A.

Molecular Determinants of Substrate Recognition in Hematopoietic Protein-tyrosine Phosphatase*

Received for publication, July 12, 2004, and in revised form, August 20, 2004
Published, JBC Papers in Press, October 4, 2004, DOI 10.1074/jbc.M407820200

Zhonghui Huang, Bo Zhou, and Zhong-Yin Zhang‡

From the Department of Molecular Pharmacology, Albert Einstein College of Medicine, Bronx, New York 10461

The extracellular signal-regulated protein kinase 2 (ERK2) plays a central role in cellular proliferation and differentiation. Full activation of ERK2 requires dual phosphorylation of Thr^{183} and Tyr^{185} in the activation loop. Tyr^{185} dephosphorylation by the hematopoietic protein-tyrosine phosphatase (HePTP) represents an important mechanism for down-regulating ERK2 activity. The bisphosphorylated ERK2 is a highly efficient substrate for HePTP with a k_{cat}/K_m of 2.6×10^6 M^{-1} s^{-1}. In contrast, the k_{cat}/K_m values for the HePTP-catalyzed hydrolysis of Tyr(P) peptides are 3 orders of magnitude lower. To gain insight into the molecular basis for HePTP substrate specificity, we analyzed the effects of altering structural features unique to HePTP on the HePTP-catalyzed hydrolysis of *p*-nitrophenyl phosphate, Tyr(P) peptides, and its physiological substrate ERK2. Our results suggest that substrate specificity is conferred upon HePTP by both negative and positive selections. To avoid nonspecific tyrosine dephosphorylation, HePTP employs Thr^{106} in the substrate recognition loop as a key negative determinant to restrain its protein-tyrosine phosphatase activity. The extremely high efficiency and fidelity of ERK2 dephosphorylation by HePTP is achieved by a bipartite protein-protein interaction mechanism, in which docking interactions between the kinase interaction motif in HePTP and the common docking site in ERK2 promote the HePTP-catalyzed ERK2 dephosphorylation (~20-fold increase in k_{cat}/K_m) by increasing the local substrate concentration, and second site interactions between the HePTP catalytic site and the ERK2 substrate-binding region enhance catalysis (~20-fold increase in k_{cat}/K_m) by organizing the catalytic residues with respect to Tyr(P)^{185} for optimal phosphoryl transfer.

The mitogen-activated protein (MAP)[1] kinases are central components in cellular signaling (1–3). The extent and duration of MAP kinase activation in response to extracellular stimuli are tightly regulated in a cell type- and stimulus-dependent manner, because of the coordinated action of protein kinases and phosphatases. Full activation of the MAP kinases requires dual phosphorylation of the Thr and Tyr residues in the activation loop by specific MAP kinase kinases. Down-regulation of MAP kinase activity is carried out by multiple protein phosphatases, including Ser/Thr-specific, Tyr-specific, and dual specificity phosphatases (4). This would inevitably lead to the formation of monophosphorylated MAP kinases. Indeed, recent evidence indicates that both forms of the monophosphorylated extracellular signal-regulated kinase 2 (ERK2), a founding member of the MAP kinase family, exist in living cells, in addition to the bisphosphorylated and unphosphorylated forms (5, 6). Interestingly, the activity of the monophosphorylated ERK2/pY and ERK2/pT is ~2 and 3 orders of magnitude higher than that of the unphosphorylated ERK2 and is only 1 and 2 orders of magnitude lower than that of the fully active bisphosphorylated ERK2/pTpY (7). This raises the possibility that the monophosphorylated ERK2s may have distinct biological roles *in vivo*.

There is considerable complexity in the regulation of ERK2 activity by protein phosphatases. Partial ERK2 inactivation can occur through the action of protein Ser/Thr phosphatase PP2A, which targets the Thr(P) in the activation loop, resulting in an ~100-fold decrease in ERK2 kinase activity (4, 7). Complete ERK2 inactivation can be accomplished by the dual specificity MAP kinase phosphatase 3 (MKP3), which is capable of removing phosphoryl groups from both Thr(P) and Tyr(P) (8, 9). In addition to PP2A and MKP3, biochemical studies suggest that distinct protein-tyrosine phosphatases (PTPs) are also involved in ERK2 inactivation (10, 11). In budding yeast, *Saccharomyces cerevisiae*, the mating pheromone-induced activation of MAP kinase Fus3 and Kss1 is tightly regulated by the concerted action of the dual specificity phosphatase Msg5 and the PTPs, Ptp2 and Ptp3 (12). Genetic and biochemical analyses have shown that the tyrosine-specific phosphatase, PTP-ER, functions to directly down-regulate ERK activity during *Drosophila* eye development (13). The mammalian orthologs of the *Drosophila* PTP-ER include the hematopoietic PTP HePTP (also known as leukocyte PTP) (14) and the brain-specific PTPs STEP (striatum-enriched PTP) (15) and PTP-SL (STEP-like PTP) (16). Indeed, recent biochemical studies indicate that HePTP, STEP, and PTP-SL negatively regulate the ERK2 pathway by dephosphorylation of Tyr(P)^{185} in the activation loop of ERK2 (17–23), resulting in a 10-fold decrease in ERK2 kinase activity (7, 24). The fact that multiple phosphatases are involved in the regulation of MAP kinase suggests that phosphatases may play a crucial role in controlling cellular responses to external stimuli and determining the time course, threshold for activation, and efficiency of MAP kinase signaling.

Although the PTPs have conserved catalytic domains and share a common mechanism of action (hydrolysis of Tyr(P))

* This work was supported by National Institutes of Health Grant CA69202 and by the G. Harold and Leila Y. Mathers Charitable Foundation. The costs of publication of this article were defrayed in part by the payment of page charges. This article must therefore be hereby marked "*advertisement*" in accordance with 18 U.S.C. Section 1734 solely to indicate this fact.

‡ To whom correspondence should be addressed: Dept. of Molecular Pharmacology, Albert Einstein College of Medicine, 1300 Morris Park Ave., Bronx, NY 10461. Tel.: 718-430-4288; Fax: 718-430-8922; E-mail: zyzhang@aecom.yu.edu.

[1] The abbreviations used are: MAP, mitogen-activated protein; ERK, extracellular signal-regulated protein kinase; MKP, MAP kinase phosphatase; PTP, protein-tyrosine phosphatase; HePTP, hematopoietic PTP; *p*NPP, *p*-nitrophenyl phosphate; KIM, kinase interaction motif; CD, common docking.

(25), the cellular processes in which they are involved can be both highly specialized and fundamentally important, in large part because of the distinct substrate specificity of individual PTPs. Thus, to fully understand the role of PTPs in signal transduction, it is necessary to have a detailed understanding of how they recognize their substrate. Recently, we carried out a rigorous kinetic analysis of ERK2/pTpY dephosphorylation by 11 protein phosphatases, many of which were previously implicated to be involved in ERK2 regulation (4). Only PP2A, MKP3, and HePTP were found to be likely ERK2 phosphatases. The k_{cat}/K_m value for the HePTP-catalyzed ERK2 dephosphorylation is 2.2×10^6 M^{-1} s^{-1}, which is similar to those of PP2A and MKP3, indicating that ERK2/pTpY is a highly efficient substrate for HePTP. In contrast, the k_{cat}/K_m of the prototypical PTPs, PTP1B and CD45, toward ERK2 is 2–3 orders of magnitudes lower than that of HePTP. These results provide biochemical evidence that PTPs display exquisite specificity in their substrate recognition. However, how HePTP achieves its substrate specificity at the molecular level is not well understood. To gain insight into this question, we studied the effects of altering amino acids unique to HePTP on ERK2 dephosphorylation catalyzed by HePTP. We have identified structural features in HePTP that mediate specific ERK2 recognition and inactivation as well as elements that prevent nonspecific Tyr(P) dephosphorylation by HePTP.

EXPERIMENTAL PROCEDURES

Expression and Purification of HePTP and Its Mutants—The coding sequence for the full-length HePTP and the NH_2-terminal truncated HePTP/Δ31 were produced by PCR using pGEX-3X-HePTP360 as a template (7). For the full-length HePTP, the oligonucleotides GCCCATATGACCCAGCCTCCGCCTGA (NdeI site underlined) and GCGGATCCTCAGGGGCTGGGTTCCT (BamHI site underlined) were used as the 5′ and 3′ primers, respectively. For HePTP/Δ31, the 5′ primer was GCCCATATGTCCCTGGGGGCCGTAGA (NdeI site underlined), and the 3′ primer was the same as that for the full-length HePTP. The PCR products containing the 5′ NdeI site and 3′ BamHI site were subcloned into pET28a vector (Novagen). All of the point mutants of HePTP were generated by PCR using the QuikChange™ site-directed mutagenesis kit (Stratagene) with pET28a-HePTP as the template. All of the mutations were confirmed by DNA sequencing.

To produce the HePTP(1–71)-PTP1B(1–321) chimera, the plasmid pET28a-HePTP(1–71)-GT-PTP1B(1–321) was constructed by a QuikChange PCR using pET28a-HePTP as template and oligonucleotides CAGCGCCAGCCACCC**GGTACC**AAGCAACTGGAAG and CTTCCAGTTGCTT**GGTACC**GGGTGGCTGGCGCTG (KpnI site underlined, mutated nucleotide in bold) as primers, to create a KpnI site in HePTP coding sequence (nucleotide 214, 216, and 217 mutated). The resulting mutant pET28a-HePTP/S72G/P73T was subjected to KpnI/BamHI digestion, and the larger DNA fragment (~5.5 kb) was recovered, resulting in the removal of the coding sequence for HePTP residues 73–339. For the second half of the chimera, PCR was performed to amplify the coding sequence for PTP1B residues 1–321, using pT7–7-PTP1B(1–321) (26) as the template and oligonucleotides CCCCGGTACCATGGAGATGGAAAAGGAGTTCGAGC (KpnI site underlined) and GACTCTAGAGGATCCCCGGGCGCG (BamHI site underlined) as the 5′ and 3′ primers, respectively. The PCR product was subjected to KpnI/BamHI digestion and ligated with the HePTP DNA fragment mentioned above, yielding an expression vector for NH_2-terminal His-tagged HePTP-PTP1B chimera HePTP(1–71)-Gly-Thr-PTP1B(1–321). Another chimera HePTP(1–35)-PTP1B(1–321) expression vector pET28a-HePTP(1–35)-Thr-PTP1B(1–321) was constructed in the same way as that of the plasmid pET28a-HePTP(1–71)-Gly-Thr-PTP1B(1–321). All of the constructs were verified by DNA sequencing.

The NH_2-terminal His_6-tagged HePTP and its mutants as well as HePTP-PTP1B chimeras were expressed in *Escherichia coli* and purified using the standard procedures of nickel chelate affinity chromatography. Protein concentration was determined using a Bradford dye binding assay (Advanced Protein Assay Reagent, Cytoskeleton Inc.) according to the manufacturer's recommendations. PTP1B and its mutants were expressed and purified as previously described (26). The purified protein was made to 30% glycerol and stored at −80 °C.

Preparation of ERK2/pTpY—The recombinant kinase inactive His_6-ERK2/K52R was purified and phosphorylated by a constitutively active MEK1 (MEK1/G7B) (27) as previously described (9) except that no radioactive ATP was used. After the dialysis against 50 mM NaCl in buffer A (20 mM Tris, 1 mM EDTA, 10% glycerol, pH 7.4), the phosphorylated ERK2 was purified by a MonoQ HR5/5 column and was eluted by a NaCl gradient from 50 to 400 mM in buffer A. The fractions of peak 1 (form 120 to 150 mM NaCl) were pooled, concentrated, and stored at −80 °C. The stoichiometry of the bisphosphorylated ERK2/K52R/pTpY was assessed using procedures similar to those described previously (7).

Determination of Kinetic Parameters Using pNPP, Tyr(P)-containing Peptides, and ERK2/pTpY as Substrates—Kinetic parameters for the PTP-catalyzed hydrolysis of *p*NPP were determined at 30 °C in pH 7 buffer containing 50 mM 3,3-dimethylglutarate, 1 mM EDTA with an ionic strength of 150 mM adjusted by addition of NaCl as described previously (4). The hydrolysis of Tyr(P)-containing peptides catalyzed by PTP was measured using a continuous spectrophotometric or fluorimetric assay as previously described (28). All of the assays were conducted at 30 °C and in the same assay buffer as the *p*NPP assay. For HePTP and its mutants other than D236A, 20–80 μM of the phosphotyrosine-containing peptides were used, which was much less than the K_m values. When the enzyme concentration used was greatly less than substrate concentration, the reaction is first order with respect to substrate concentration, the k_{cat}/K_m value for the phosphatase was obtained by fitting the progress curve to Equation 1.

$$[P] = [S] \times [1 - e^{-(k_{cat}/K_m)\times[E]\times t}] \quad \text{(Eq. 1)}$$

For PTP1B and HePTP-PTP1B chimeras, the Tyr(P)-containing peptide concentrations were from 50 to 100 μM, which was greatly larger than the K_m values. When enzyme concentration used was greatly less than substrate concentration, the k_{cat} and K_m values for the enzyme were obtained by fitting the progress curves to Equation 2.

$$t = p/k_{cat}E + (K_m/k_{cat}E) \ln [p_\infty/(p_\infty - p)] \quad \text{(Eq. 2)}$$

Because the k_{cat} and K_m for HePTP/D236A are much lower than those of the wild-type enzyme, the kinetic parameters for the HePTP/D236A-catalyzed Tyr(P) peptide hydrolysis were determined using an enzyme-coupled continuous spectrophotometric assay (7). The peptide concentration ranged from 0.2 to 5 K_m. Because the enzyme concentration used was comparable with that of substrate concentration in this experiment, the kinetic parameters were obtained from a fit of the initial velocity *versus* substrate concentration data to Equation 3.

$$v = 0.5 \times k_{cat} \times \{(K_m + [E] + [S]) - (K_m + [E] + [S])^2 - 4 \times [E] \times [S]]^{1/2}\} \quad \text{(Eq. 3)}$$

Kinetic parameters for the dephosphorylation of the phosphorylated ERK2 protein were determined using a continuous spectrophotometric assay described previously (4, 29).

RESULTS AND DISCUSSION

HePTP is a cytosolic enzyme of hematopoietic origin that is most similar to the brain-specific PTPs STEP and PTP-SL (Fig. 1). Sequence analysis suggests that the catalytic domains of HePTP, STEP, and PTP-SL possess all of the invariant residues characterizing the PTP family. Many of these invariant residues are important for either catalysis and/or structural integrity (25), and they are unlikely to confer PTP substrate specificity. In addition, the crystal structure of the catalytic domain of PTP-SL encompassing residues 254–549, which correspond to residues 44–338 in HePTP, highly resembles those of other PTPs (30). Given the overall structural similarities of the PTP-SL catalytic domain to other PTPs, it is uncertain what are the molecular determinants for specific ERK2 dephosphorylation by this group of PTPs. A unique property of the HePTP subfamily of PTPs is the existence of a kinase interaction motif (KIM, residues 17–30 in HePTP) NH_2-terminal to the catalytic domain that is directly involved in ERK2 binding (17, 19, 22). Because the crystal structure of PTP-SL does not include the KIM sequence (30), it is unclear how KIM contributes to the specificity of HePTP toward ERK2. Finally, it is also not known how HePTP avoids nonspecific dephosphorylation of Tyr(P)-containing proteins other than ERK2.

To begin to delineate the molecular determinants for HePTP

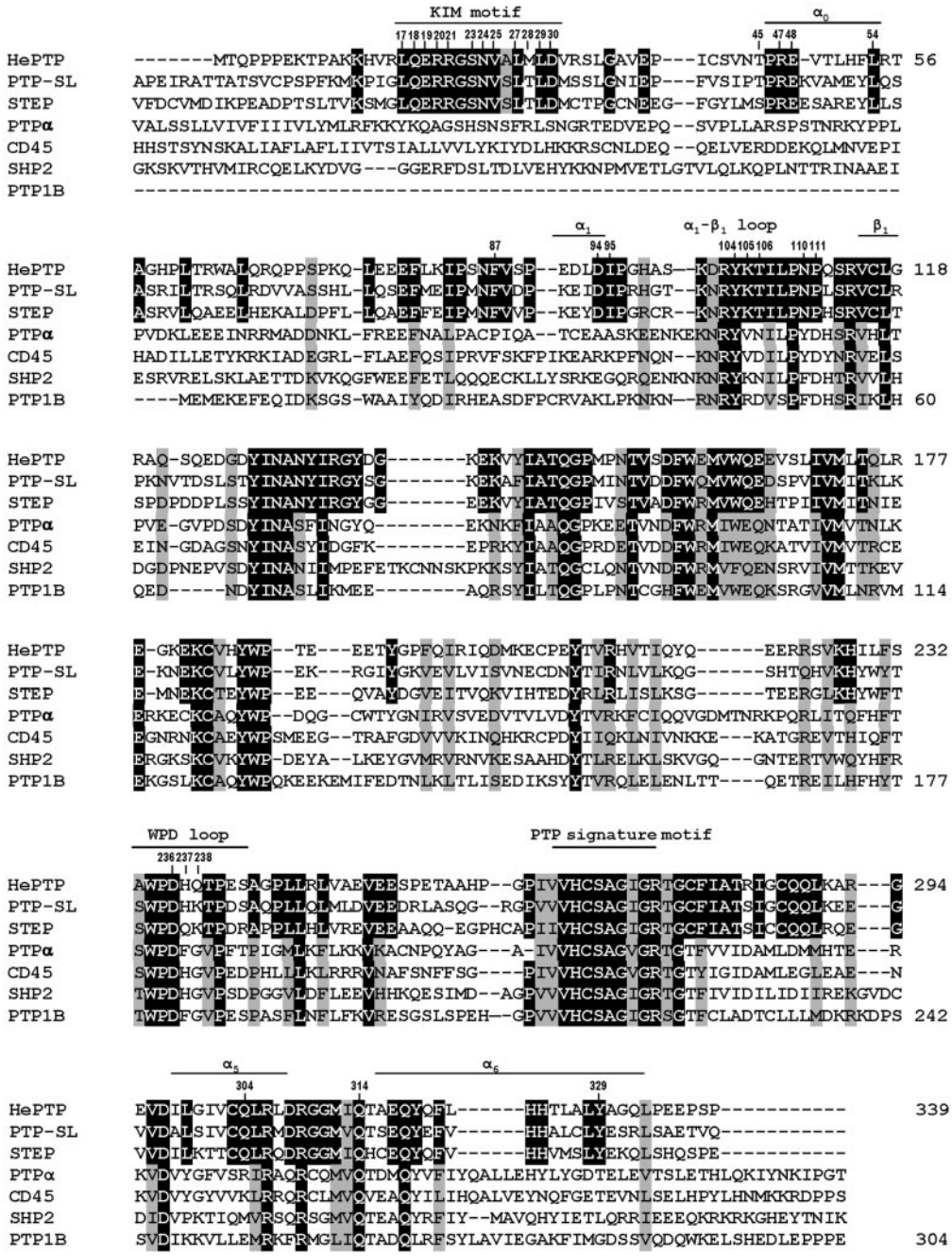

FIG. 1. **Amino acid sequence alignment of HePTP (full-length, residues 1–339), PTP-SL (residues 310–657), STEP (residues 188–537), PTPα (residues 148–528), CD45 (residues 567–937), SHP2 (residues 163–546), and PTP1B (residues 1–304).** The *letters* in the *black boxes* represent either residues that are absolutely invariant among all PTPs or residues that are unique to HePTP, PTP-SL, and STEP. The *letters* in *shaded boxes* indicate conserved substitutions. The secondary structure designations are as defined in Ref. 30. HePTP residues that were subjected to mutagenesis are *numbered*.

substrate recognition, we decided to focus on amino acid residues that are unique to HePTP, STEP, and PTP-SL (Fig. 1). Specifically, we carried out site-directed mutagenesis of HePTP in the KIM sequence (residues 17–30), α_0 helix (residues 48–55), α_1-β_1 loop (residues 85–112), the WPD loop (residues 232–243), α_5 helix (residues 298–308), α_5-α_6 loop (residues 309–315), and α_6 helix (residues 316–331). The KIM sequence is important for ERK2 binding (17, 19, 21, 22, 31). The α_0 helix is unique to PTP-SL, which connects the KIM motif with the PTP domain (30). The α_1-β_1 loop is the substrate recognition loop involved in binding of Tyr(P)-containing peptides in PTP1B (32–34). The WPD loop, α_5, α_5-α_6 loop, and α_6 are structural elements that surround the active site. In addition, we also prepared chimeric molecules in which the NH_2-terminal segment of HePTP including the KIM sequence was fused to the catalytic domain of PTP1B.

Effect of Mutations in HePTP on pNPP Hydrolysis—Wild-type and mutant HePTPs were expressed in *E. coli* and purified to near homogeneity as judged by SDS-PAGE. We first evaluated the effects of amino acid substitutions in HePTP using *p*NPP as a substrate. All of the kinetic measurements were conducted at 30 °C in pH 7.0, 50 mM 3,3-dimethylglutarate buffer, containing 1 mM EDTA with an ionic strength of 0.15 M. The kinetic parameters for the wild-type and mutant HePTP-catalyzed *p*NPP hydrolysis are listed in Table I. Although the k_{cat} and k_{cat}/K_m values for HePTP are several fold lower than those of PTP1B, the most thoroughly characterized prototypical PTP, they are within the range observed for mammalian

TABLE I
*Kinetic parameters of HePTP and its mutants with p*NPP as a substrate at pH 7 and 30 °C

HePTP	Mutation	k_{cat}	K_m	k_{cat}/K_m
		s^{-1}	mM	$M^{-1}\ s^{-1}$
Wild type	None	3.81 ± 0.21	7.44 ± 0.83	(5.12 ± 0.58) × 10^2
KIM (17–30)	ΔN 31	4.20 ± 0.04	6.15 ± 0.30	(6.83 ± 0.34) × 10^2
	L17A	4.12 ± 0.16	8.13 ± 0.66	(5.07 ± 0.32) × 10^2
	Q18A	4.60 ± 0.25	11.50 ± 1.49	(4.00 ± 0.41) × 10^2
	E19A	3.70 ± 0.11	9.51 ± 0.60	(3.89 ± 0.25) × 10^2
	R20A	4.55 ± 0.21	9.99 ± 1.18	(4.55 ± 0.41) × 10^2
	R21A	4.95 ± 0.21	10.02 ± 1.03	(4.94 ± 0.51) × 10^2
	R20A/R21A	3.09 ± 0.08	6.50 ± 0.44	(4.75 ± 0.33) × 10^2
	S23D	6.78 ± 0.29	7.24 ± 0.69	(9.36 ± 0.89) × 10^2
	N24A	7.45 ± 0.33	7.52 ± 0.73	(9.91 ± 0.96) × 10^2
	V25A	2.39 ± 0.18	12.21 ± 2.55	(1.96 ± 0.41) × 10^2
	L27A	5.74 ± 0.33	9.44 ± 1.11	(6.08 ± 0.72) × 10^2
	M28A	7.54 ± 0.34	12.78 ± 1.42	(5.90 ± 0.66) × 10^2
	L29A	5.42 ± 0.30	9.98 ± 1.39	(5.43 ± 0.76) × 10^2
	D30A	5.53 ± 0.28	8.46 ± 0.94	(6.55 ± 0.73) × 10^2
α_0 (48–55)	T45E	5.73 ± 0.21	2.78 ± 0.23	(2.06 ± 0.17) × 10^3
	R47A	6.00 ± 0.33	11.23 ± 1.50	(5.34 ± 0.54) × 10^2
	E48A	4.56 ± 0.27	9.63 ± 0.99	(4.74 ± 0.49) × 10^2
	L54A	2.21 ± 0.19	11.7 ± 1.94	(1.89 ± 0.26) × 10^2
α_1-β_1 loop (85–112)	F87A	2.78 ± 0.31	6.72 ± 0.81	(4.14 ± 0.50) × 10^2
	D94A	3.68 ± 0.40	6.20 ± 0.38	(5.94 ± 0.53) × 10^2
	I95A	2.97 ± 0.16	6.01 ± 0.61	(4.94 ± 0.51) × 10^2
	Y104A	0.162 ± 0.019	12.63 ± 1.70	12.8 ± 1.7
	K105A	4.34 ± 0.24	9.66 ± 1.03	(4.50 ± 0.49) × 10^2
	T106A	4.25 ± 0.21	6.91 ± 0.35	(6.15 ± 0.32) × 10^2
	T106D	5.23 ± 0.45	12.63 ± 1.89	(4.14 ± 0.62) × 10^2
	T106N	3.44 ± 0.17	7.99 ± 0.73	(4.31 ± 0.40) × 10^2
	T106V	2.09 ± 0.08	7.54 ± 0.55	(2.77 ± 0.21) × 10^2
	T106S	4.10 ± 0.12	6.42 ± 0.44	(6.39 ± 0.44) × 10^2
	T106L	2.12 ± 0.12	5.25 ± 0.74	(5.56 ± 0.78) × 10^2
	N110A	2.67 ± 0.13	9.57 ± 0.98	(2.79 ± 0.29) × 10^2
	P111A	2.71 ± 0.13	7.12 ± 0.33	(3.81 ± 0.18) × 10^2
WPD loop (232–243)	D236A	0.0103 ± 0.0004	0.586 ± 0.055	17.6 ± 1.2
	H237A	0.753 ± 0.060	7.88 ± 1.26	(9.56 ± 1.54) × 10^1
	H237F	0.562 ± 0.050	5.59 ± 1.12	(1.01 ± 0.21) × 10^2
	H237Q	1.88 ± 0.12	7.96 ± 1.03	(2.36 ± 0.31) × 10^2
	Q238G	3.08 ± 0.15	6.95 ± 0.71	(4.43 ± 0.45) × 10^2
α_5 (298–308)	Q304A	3.84 ± 0.30	8.41 ± 0.97	(4.54 ± 0.53) × 10^2
α_5-α_6 loop (309–315)	Q314A	0.454 ± 0.035	2.31 ± 0.51	(1.97 ± 0.44) × 10^2
α_6 (316–331)	Y329A	1.37 ± 0.10	9.18 ± 1.35	(1.49 ± 0.22) × 10^2

PTPs. With the exception of Y104A, D236A, H237A, H237F, and Q314A, no significant differences in the kinetic parameters for *p*NPP hydrolysis were observed between the wild-type and mutant HePTPs.

Tyr^{104} is invariant among the PTPs and is equivalent to Tyr^{46} in PTP1B, which defines the depth of the active site and is engaged in hydrophobic packing with Tyr(P) in the substrate (32). Similar to the effect observed for PTP1B/Y46A (33), replacement of Tyr^{104} with an Ala resulted in a 24-fold decrease in k_{cat} and a 40-fold decrease in k_{cat}/K_m with *p*NPP as a substrate. Asp^{236} is likely the general acid catalyst based on the sequence alignment and the crystal structure of PTP-SL. Removal of the carboxylic acid at position 236 caused a large drop in HePTP activity, which is in agreement with other general acid deficient PTPs (25). His^{237} resides in the WPD loop immediately after the general acid. In many PTPs, the corresponding residue at position 237 is a Phe (Phe^{182} in PTP1B). Previous studies showed that residues adjacent to the general acid can influence its precise positioning (35, 36). The observed effects for H237A and H237F are similar to those reported for the PTP1B Phe^{182} mutants (33, 36). Interestingly, position 237 is occupied by a Gln in STEP, rather than a His, and H237Q exhibits kinetic parameters similar to those of the wild-type HePTP. The side chains of the structurally equivalents of Gln314 in the *Yersinia* PTP (Gln^{446}) and PTP1B (Gln^{262}) function to position and activate the nucleophilic water for phosphoenzyme hydrolysis (37, 38). The sizes of reduction in k_{cat} and K_m for Q314A are similar to those observed for the *Yersinia* PTP/Q446A and PTP1B/Q262A (33, 37), suggesting that it may play a similar role in HePTP catalysis.

Because *p*NPP is a small aryl phosphate that mimics Tyr(P), its hydrolysis is sensitive only to structural perturbations to the active site. The observed effects for Y104A, D236A, H237A, H237F, and Q314A are consistent with their roles in Tyr(P) binding and/or hydrolysis. Because the KIM sequence, the α_0 helix, and the majority of the residues in the substrate recognition loop α_1-β_1 are located away from the active site and are unlikely to interact directly with Tyr(P) or *p*NPP, substitutions in these regions are not expected to have any adverse effects on the HePTP-catalyzed *p*NPP hydrolysis. The lack of changes in the kinetic parameters associated with the majority of the HePTP mutants confirms this prediction and indicates that alterations in these residues do not lead to significant structural perturbations in the HePTP active site.

Effect of Mutations in HePTP on the Dephosphorylation of Tyr(P)-containing Peptides—We next examined the effects of amino acid substitutions on the HePTP-catalyzed hydrolysis of Tyr(P)-containing peptides: QPDNVpYLVPTPS (residues 208–219 from $p130^{Cas}$), DADEpYLIPQQG (residues 988–998 from the epidermal growth factor receptor), and DHTGFLpTEpYVATR (residues 177–189 corresponding to the activation loop of ERK2). A continuous spectrophotometric assay described previously was used to follow the dephosphorylation of Tyr(P)-containing peptides (28). The values of k_{cat}/K_m for the wild-type and mutant HePTP-catalyzed dephosphorylation of the peptide substrates are listed in Table II. It appears that

TABLE II
Kinetic parameters of HePTP and its mutants with phosphopeptides as substrates at pH 7 and 30 °C

HePTP	Mutation	k_{cat}/K_m		
		QPDNVpYLVPTPS ($p130^{cas}$/208–219)	DADEpYLIPQQG (EGFR/988–998)	DHTGFLpTEpYVATR (ERK2/177–189)
		$M^{-1}\ s^{-1}$	$M^{-1}\ s^{-1}$	$M^{-1}\ s^{-1}$
Wild type	None	$(3.61 \pm 0.03) \times 10^3$	$(1.08 \pm 0.01) \times 10^4$	$(4.83 \pm 0.05) \times 10^3$
KIM (17–30)	ΔN 31	$(7.28 \pm 0.07) \times 10^3$	$(5.33 \pm 0.01) \times 10^3$	
	L17A	$(4.03 \pm 0.02) \times 10^3$	$(5.32 \pm 0.09) \times 10^3$	
	Q18A	$(5.19 \pm 0.02) \times 10^3$	$(7.78 \pm 0.08) \times 10^3$	
	E19A	$(3.38 \pm 0.01) \times 10^3$	$(6.80 \pm 0.05) \times 10^3$	
	R20A	$(3.88 \pm 0.01) \times 10^3$	$(5.33 \pm 0.04) \times 10^3$	
	R21A	$(5.17 \pm 0.02) \times 10^3$	$(1.05 \pm 0.01) \times 10^4$	
	R20A/R21A	$(3.43 \pm 0.02) \times 10^3$	$(8.99 \pm 0.01) \times 10^3$	
	S23D	$(7.46 \pm 0.02) \times 10^3$	$(1.27 \pm 0.01) \times 10^4$	
	N24A	$(8.44 \pm 0.02) \times 10^3$	$(1.56 \pm 0.01) \times 10^4$	
	V25A	$(1.12 \pm 0.01) \times 10^3$	$(1.62 \pm 0.02) \times 10^3$	
	L27A	$(6.04 \pm 0.03) \times 10^3$	$(1.29 \pm 0.01) \times 10^4$	
	M28A	$(3.94 \pm 0.01) \times 10^3$	$(1.55 \pm 0.01) \times 10^4$	
	L29A	$(3.99 \pm 0.01) \times 10^3$	$(8.07 \pm 0.08) \times 10^3$	
	D30A	$(5.13 \pm 0.02) \times 10^3$	$(6.29 \pm 0.08) \times 10^3$	
α_0 (48–55)	T45E	$(1.01 \pm 0.01) \times 10^4$	$(2.40 \pm 0.01) \times 10^4$	
	R47A	$(5.92 \pm 0.01) \times 10^3$	$(8.96 \pm 0.04) \times 10^3$	
	E48A	$(4.12 \pm 0.02) \times 10^3$	$(8.80 \pm 0.07) \times 10^3$	
	L54A	$(1.97 \pm 0.01) \times 10^3$	$(2.81 \pm 0.01) \times 10^3$	
α_1-β_1 loop (85–112)	F87A	$(1.24 \pm 0.01) \times 10^3$	$(7.40 \pm 0.01) \times 10^3$	
	D94A	$(3.86 \pm 0.03) \times 10^3$	$(1.08 \pm 0.01) \times 10^4$	
	I95A	$(3.12 \pm 0.02) \times 10^3$	$(1.18 \pm 0.01) \times 10^4$	
	Y104A	38.5 ± 0.1	34.2 ± 0.03	
	K105A	$(2.71 \pm 0.01) \times 10^3$	$(4.53 \pm 0.04) \times 10^3$	
	T106A	$(4.14 \pm 0.03) \times 10^3$	$(1.58 \pm 0.002) \times 10^4$	$(4.83 \pm 0.02) \times 10^3$
	T106D	$(1.93 \pm 0.01) \times 10^5$	$(1.16 \pm 0.01) \times 10^5$	$(2.94 \pm 0.03) \times 10^4$
	T106N	$(2.58 \pm 0.01) \times 10^5$	$(1.88 \pm 0.03) \times 10^5$	$(4.43 \pm 0.03) \times 10^4$
	T106V	$(4.69 \pm 0.03) \times 10^3$	$(6.79 \pm 0.01) \times 10^3$	$(6.13 \pm 0.03) \times 10^3$
	T106S	$(5.94 \pm 0.06) \times 10^3$	$(1.38 \pm 0.01) \times 10^4$	$(1.31 \pm 0.01) \times 10^4$
	T106L	$(8.46 \pm 0.04) \times 10^3$	$(1.32 \pm 0.003) \times 10^4$	$(9.84 \pm 0.12) \times 10^3$
	N110A	$(1.28 \pm 0.01) \times 10^3$	$(4.43 \pm 0.01) \times 10^3$	
	P111A	$(2.52 \pm 0.01) \times 10^3$	$(5.67 \pm 0.01) \times 10^3$	
WPD loop (232–243)	D236A	18.7 ± 2.4		
	H237A	$(3.14 \pm 0.01) \times 10^4$	$(1.53 \pm 0.01) \times 10^4$	
	H237F	$(4.60 \pm 0.02) \times 10^2$	$(6.40 \pm 0.06) \times 10^2$	
	H237Q	$(6.61 \pm 0.02) \times 10^2$	$(7.64 \pm 0.01) \times 10^2$	
	Q238G	$(2.72 \pm 0.02) \times 10^3$	$(5.92 \pm 0.01) \times 10^3$	
α_5 (298–308)	Q304A	$(5.79 \pm 0.03) \times 10^3$	$(1.59 \pm 0.00) \times 10^4$	
α_5-α_6 loop (309–315)	Q314A	$(1.45 \pm 0.01) \times 10^3$	$(2.10 \pm 0.01) \times 10^3$	
α_6 (316–331)	Y329A	$(1.50 \pm 0.01) \times 10^3$	$(3.89 \pm 0.01) \times 10^3$	

HePTP does not display any sequence specificity toward these peptides because the k_{cat}/K_m values for the $p130^{Cas}$, epidermal growth factor receptor, and ERK2 peptides are very similar. In addition, the k_{cat}/K_m values of HePTP toward the Tyr(P) peptides are 3 orders of magnitude lower than those of the PTP1B-catalyzed reactions (Table III). It was suggested that the low phosphatase activity of PTP-SL may be caused by a more rigid WPD loop caused by the presence of a bulky residue (Lys^{448} in PTP-SL and Gln^{238} in HePTP) in place of a Gly found in the majority of other PTPs (Ref. 30 and Fig. 1). However, no significant changes in HePTP activity were observed when Gln^{238} was replaced with a Gly residue (Tables I, II, and IV). Similar to the results obtained with *p*NPP, substitution of Tyr^{104}, Asp^{236}, and His^{237} also results in large decreases in HePTP catalytic efficiency toward the phosphopeptides. All other mutations, with the exceptions of T106D and T106N, cause little changes in the k_{cat}/K_m values for Tyr(P) peptide hydrolysis. These results indicate that the KIM sequence, the α_0 helix, and most of the residues examined in the α_1-β_1 and α_5-α_6 loops are not involved in phosphopeptide recognition. Strikingly, replacement of Thr^{106} with either an Asp or Asn results in a 10–70-fold increase in the rate of the HePTP-catalyzed phosphopeptide hydrolysis (Table II). No significant effects were observed when Thr^{106} was changed to an Ala, a Val, a Ser, or a Leu.

Thr^{106} resides in the PTP substrate recognition loop α_1-β_1 and is conserved among HePTP, STEP, and PTP-SL (Fig. 1). Interestingly, in all other PTPs this position is either an Asp or Asn. In PTP1B, the corresponding residue is Asp^{48}, which makes two hydrogen bonds to the main chain nitrogens of Tyr(P) and the +1 residue in the peptide substrate (32, 34). Similar to our previous findings (33), substitution of Asp^{48} in PTP1B by an Ala led to a 40–80-fold decrease in k_{cat}/K_m for the peptide substrates, whereas the more conservative Asp^{48} to Thr change resulted in a 10–30-fold drop in the k_{cat}/K_m values (Table III). The magnitudes of reduction in k_{cat}/K_m for the PTP1B D48A and D48T-catalyzed hydrolysis of Tyr(P) peptides are consistent with the abrogation of two hydrogen bonds between the carboxyl group of Asp^{48} and the main chain nitrogens of Tyr(P) and the +1 residue in the peptide substrate. These same mutations have no adverse effects on the hydrolysis of *p*NPP, which lacks the corresponding main chain nitrogens. Based on the structural and biochemical data, we propose that an Asp (or Asn) at this position may be essential for efficient dephosphorylation of Tyr(P)-containing substrates by the PTPs. This notion is supported by the fact that the HePTP-catalyzed phosphopeptide hydrolysis can be enhanced 10–70-fold by the reciprocal mutation of Thr^{106} to either an Asp or Asn. Thus, Thr^{106} may serve as a negative determinant to curb the phosphatase activity of HePTP toward nonspecific Tyr(P)-containing substrates. It is also worth noting that although Arg^{47} in PTP1B is engaged in numerous interactions with the

TABLE III
Kinetic parameters of HePTP, PTP1B, and HePTP/PTP1B chimera with pNPP, phosphopeptides, and ERK2/pTpY as substrates at pH 7 and 30 °C

HePTP/PTP1B Chimera	*p*NPP as a substrate		
	k_{cat}	K_m	k_{cat}/K_m
	s^{-1}	mM	$M^{-1}\ s^{-1}$
HePTP	3.81 ± 0.21	7.44 ± 0.83	(5.12 ± 0.58) × 10^2
PTP1B	19.2 ± 0.7	2.08 ± 0.19	(9.21 ± 0.84) × 10^3
PTP1B/D48A	12.8 ± 0.2	1.26 ± 0.06	(1.02 ± 0.05) × 10^4
PTP1B/D48T	15.6 ± 1.2	1.63 ± 0.31	(9.57 ± 1.43) × 10^3
HePTP(1–35)/PTP1B	12.83 ± 0.44	2.37 ± 0.21	(5.41 ± 0.36) × 10^3
HePTP(1–71)/PTP1B	10.38 ± 0.37	2.00 ± 0.14	(5.19 ± 0.31) × 10^3
HePTP(1–71)/PTP1B/D48T	5.26 ± 0.18	1.09 ± 0.13	(4.83 ± 0.58) × 10^3

HePTP/PTP1B Chimera	Phosphopeptides as substrates (k_{cat}/K_m)		
	QPDNVpYLVPTPS ($p130^{Cas}$/208–219)	DADEpYLIPQQG (EGFR/988–998)	DHTGFLpTEpYVATR (ERK2/177–189)
	$M^{-1}\ s^{-1}$	$M^{-1}\ s^{-1}$	$M^{-1}\ s^{-1}$
HePTP	(3.61 ± 0.03) × 10^3	(1.08 ± 0.01) × 10^4	(4.83 ± 0.05) × 10^3
PTP1B	(6.84 ± 0.04) × 10^6	(8.32 ± 0.08) × 10^6	(3.41 ± 0.10) × 10^6
PTP1B/D48A	(8.61 ± 0.05) × 10^4	(2.02 ± 0.05) × 10^5	
PTP1B/D48T	(2.54 ± 0.02) × 10^5	(6.89 ± 0.45) × 10^5	
HePTP(1–35)/PTP1B	(2.46 ± 0.04) × 10^6	(4.37 ± 0.15) × 10^6	
HePTP(1–71)/PTP1B	(1.75 ± 0.02) × 10^6	(4.89 ± 0.14) × 10^6	(1.42 ± 0.10) × 10^6
HePTP(1–71)/PTP1B/D48T	(2.24 ± 0.06) × 10^5	(2.44 ± 0.02) × 10^5	

HePTP/PTP1B Chimera	ERK2/pTpY as a Substrate		
	k_{cat}	K_m	k_{cat}/K_m
	s^{-1}	μM	$M^{-1}\ s^{-1}$
HePTP	1.59 ± 0.11	0.61 ± 0.11	(2.61 ± 0.51) × 10^6
PTP1B		>2	(6.48 ± 0.04) × 10^3
PTP1B/D48A		>2	(1.29 ± 0.10) × 10^3
PTP1B/D48T		>2	(1.98 ± 0.12) × 10^3
HePTP(1–35)/PTP1B	0.202 ± 0.019	1.37 ± 0.28	(1.48 ± 0.30) × 10^5
HePTP(1–71)/PTP1B	0.13 ± 0.01	1.23 ± 0.14	(1.06 ± 0.12) × 10^5
HePTP(1–71)/PTP1B/D48T	0.043 ± 0.004	0.82 ± 0.26	(5.25 ± 1.66) × 10^4

−1, −2, and −4 positions in Tyr(P)-containing peptides (32, 34), the structurally equivalent Lys^{105} in HePTP is not required for Tyr(P) peptide dephosphorylation. Collectively, the data with phosphopeptides suggest that HePTP may have adopted a substrate recognition strategy significantly different from that used by PTP1B.

Effect of Mutations in HePTP on ERK2 Dephosphorylation—To gain further insight into the molecular basis of HePTP substrate specificity, we analyzed the HePTP-catalyzed dephosphorylation of its physiological substrate ERK2. We showed previously that HePTP can dephosphorylate both the monophosphorylated ERK2/pY and the bisphosphorylated ERK2/pTpY with similar efficiency, indicating that dephosphorylation of Tyr(P) in ERK2 by HePTP does not require the presence of Thr(P) in the activation loop (4). We prepared bisphosphorylated ERK2 with both the wild-type and the catalytically impaired K52R mutant ERK2 by *in vitro* phosphorylation with a constitutively active form of MEK1 (MEK1/G7B) (9, 27). We found that it was easier to achieve full phosphorylation stoichiometry with ERK2/K52R than with the wild-type ERK2, possibly because of the lower ATPase activity of the mutant (39). The homogeneity and phosphorylation stoichiometry of the bisphosphorylated ERK2 preparations were verified by SDS-PAGE and liquid chromatography-mass spectrometry as described previously (4, 7, 9). Analysis of the HePTP-catalyzed dephosphorylation of the bisphosphorylated wild-type ERK2 and the K52R mutant yielded identical kinetic constants. Similarly, kinetic constants obtained for the MKP3-catalyzed ERK2 dephosphorylation are also indistinguishable from those using ERK2/K52R as a substrate (9). Thus, results described in this report were obtained using the kinase-impaired ERK2/K52R mutant as a HePTP substrate.

To follow the HePTP-catalyzed Tyr(P) hydrolysis in ERK2/pTpY, we employed a continuous spectrophotometric enzyme-coupled assay in which the coupling enzyme purine nucleoside phosphorylase uses the inorganic phosphate, generated by the action of HePTP, to convert 7-methyl-6-thioguanosine to 7-methyl-6-thioguanine and ribose-1-phosphate, resulting in an increase in absorbance at 360 nm (4, 29). Fig. 2 shows a typical progress curve of the HePTP-catalyzed ERK2/pTpY dephosphorylation. Only one equivalent of inorganic phosphate was released upon treatment of ERK2/pTpY with HePTP. Subsequent addition of MKP3, a dual specificity phosphatase for ERK2 (9), produced another equivalent of inorganic phosphate, most likely from the hydrolysis of the remaining ERK2/pT. By fitting the initial rates *versus* [ERK2/pTpY] data to the Michaelis-Menten equation (Fig. 3), the k_{cat} and K_m values for the HePTP-catalyzed dephosphorylation of ERK2/pTpY were determined to be 1.59 ± 0.11 s^{-1} and 0.61 ± 0.11 μM, respectively, at pH 7.0 and 30 °C (Table IV). These values are similar to those measured in an early study under comparable conditions (4). The k_{cat}/K_m value for the HePTP-catalyzed ERK2 dephosphorylation is 2.61 × 10^6 $M^{-1}\ s^{-1}$, indicating that ERK2/pTpY is a highly efficient substrate for HePTP.

Although PTP1B is more efficient than HePTP in hydrolyzing *p*NPP and Tyr(P)-containing peptides, its k_{cat}/K_m value for ERK2/pTpY dephosphorylation is 400-fold lower than that of the HePTP-catalyzed reaction (Table III). In fact, the k_{cat}/K_m value for the PTP1B-catalyzed ERK2/pTpY dephosphorylation is similar to that for the *p*NPP reaction and 3 orders of magnitude lower that those for the peptide substrates. Thus, unlike results with phosphopeptides, which suggest that PTPs only exhibit moderate sequence specificity, the results described here and from an earlier study (4) with ERK2/pTpY demonstrate that PTPs exhibit extremely high substrate specificity toward protein substrates.

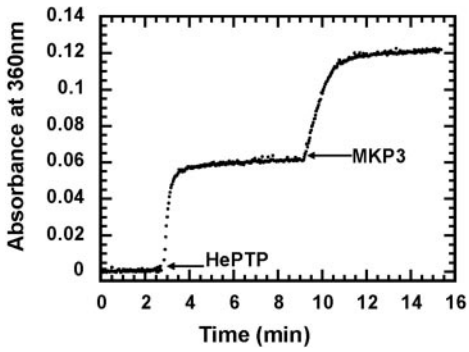

FIG. 2. **The time courses of ERK2/pTpY dephosphorylation by HePTP and MKP3.** The reaction containing 5.4 μM ERK2/pTpY was initiated by addition of 100 nM HePTP, followed by 500 nM MKP3. The phosphate released from ERK2 was monitored by the increase in absorbance at 360 nm in the presence of 50 μM 7-methyl-6-thioguanosine, 0.1 mg/ml purine nucleoside phosphorylase in 100 mM Tris, pH 7.0, 150 mM NaCl, 1 mM EDTA at 30 °C.

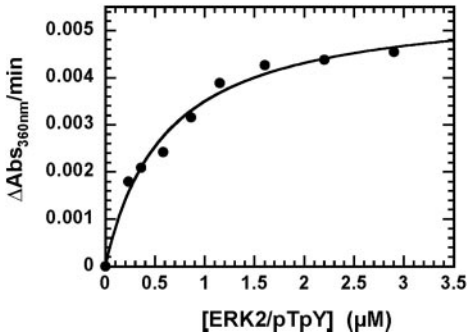

FIG. 3. **Dependence of the initial velocity (ΔAbs_{360}/min) on ERK2/pTpY concentration for the HePTP-catalyzed reaction.** All of the experiments were performed at 30 °C and pH 7.0 in 100 mM Tris, 150 mM NaCl, 1 mM EDTA. The reaction was initiated by the addition of 5 nM HePTP to the mixture. The inorganic phosphate released form ERK2/pTpY during the HePTP catalyzed dephosphorylation was determined continuously by the coupled enzyme assay (see "Experimental Procedures"). The data were fitted to the Michaelis-Menten equation to obtain the K_m and k_{cat} values.

We hypothesized that both variable residues in the catalytic domain and unique sequence motifs outside of the catalytic domain contribute to HePTP substrate specificity. To test this hypothesis, we analyzed ERK2/pTpY dephosphorylation by both the wild-type and mutant HePTPs (Table IV). More than 2,800-fold reduction in k_{cat} and >10-fold decrease in K_m were observed for the HePTP/D236A mutant. The diminished activity of HePTP/D236A toward ERK2/pTpY is consistent with Asp^{236} functioning as a general acid. The decrease in K_m is in line with previous observations that the Asp to Ala general acid deficient PTP possesses an enhanced affinity for substrates (40–43). Removal of the side chain from Tyr^{104} led to 55- and 130-fold decreases in k_{cat} and k_{cat}/K_m, respectively. Thus, similar to the *p*NPP and phosphopeptide reactions, proper positioning of Tyr(P) in the active site is critical for efficient ERK2 dephosphorylation by HePTP. Surprisingly, aside from Tyr^{104}, mutations of residues in the α_1-β_1 substrate recognition loop, including Phe^{87}, Asp^{94}, Ile^{95}, Thr^{106}, Asn^{110}, and Pro^{111} that are unique to the HePTP subfamily, do not affect the ability of HePTP to dephosphorylate ERK2/pTpY. Moreover, alterations of several HePTP-specific residues in the WPD loop (Gln^{238}), α_5 (Gln^{304}), and α_6 (Tyr^{329}) also have no effect on ERK2 dephosphorylation by HePTP. Thus, none of the residues selected for mutagenesis in the HePTP catalytic domain serve as specificity determinants for ERK2 substrate recognition.

Because the k_{cat}/K_m (also called the substrate specificity constant) for the HePTP-catalyzed ERK2/pTpY dephosphorylation is nearly 3 orders of magnitude higher than that for DHTGFLpTEpYVATR, a phosphopeptide derived from the ERK2 activation loop containing both $Thr(P)^{183}$ and $Tyr(P)^{185}$, it is clear that local interactions involving HePTP active site and its immediate surroundings with the phosphopeptide are insufficient to confer its specificity for ERK2. Thus, specific recognition of ERK2 by HePTP may involve its NH_2-terminal noncatalytic segment (residues 1–70), in addition to the active site interactions that engage the phosphoamino acid residue in ERK2. Indeed, it has been shown that a segment containing the KIM sequence (residues 17–31 in HePTP; Fig. 1) NH_2-terminal to the catalytic domain of HePTP and PTP-SL is essential for ERK2 binding and inactivation in transient transfection experiments (17, 19, 21, 22), and the KIM peptide from HePTP binds ERK2 with a K_d of 5 μM (31). The KIM sequence is characterized by a cluster of positively charged residues and is present in many ERK2-binding proteins, including its regulators and substrates (13, 17, 19, 31, 44–47). Evidence suggests that the KIM sequence mediates ERK2 binding through specific protein-protein interactions with an acidic common docking (CD) domain (residues 311–324 in ERK2) distant from the phosphorylation sites (44, 48, 49).

To assess the contribution of the NH_2-terminal noncatalytic segment to HePTP-catalyzed ERK2/pTpY dephosphorylation, we examined the effects of structural perturbations to both the KIM sequence and the α_0 helix (residues 48–55 in HePTP), a secondary structural element that is unique to the KIM-containing PTPs. The crystal structure of PTP-SL revealed that α_0 follows an ERK2 phosphorylation site (Thr^{45}) and provides several solvent exposed residues (Arg^{47}, Glu^{48}, and Leu^{54}) likely forming a putative ligand-binding site (30). Based on the structure, it was also suggested that α_0 may also be important for the relative orientation of the KIM sequence and the PTP catalytic domain. Our data indicate that neither the KIM sequence nor the α_0 helix is important for the intrinsic activity of HePTP toward *p*NPP or phosphopeptides (Tables I and II). As evident from Table IV, substitution of Thr^{45} by an acidic Glu residue or removal of side chains from Arg^{47}, Glu^{48}, and Leu^{54} had no apparent effect on the HePTP-catalyzed ERK2 dephosphorylation. In contrast, when residues 1–31 were removed from HePTP, the resulting HePTP/ΔN31 displayed a k_{cat}/K_m for ERK2 dephosphorylation that was 214-fold lower than that of the wild-type enzyme (Table IV). This is consistent with the finding that the KIM motif is important for high affinity ERK2 binding.

We then assessed the importance of individual residues in the KIM sequence for ERK2 dephosphorylation by HePTP. When the Arg residues at positions 20 and 21 were replaced by an Ala, the k_{cat}/K_m of R20A and R21A for ERK2 dephosphorylation decreased 7.7 and 2.7-fold, respectively. Interestingly, replacement of both Arg20 and Arg21 with an Ala led to an 86-fold drop in the k_{cat}/K_m value, indicating a negative cooperativity in binding between these two arginines. A reduction of k_{cat}/K_m in the range of 4–38-fold was also observed upon removal of hydrophobic side chains from Leu^{17}, Val^{25}, Leu^{27}, and Leu^{29} (Table IV). Thus, Leu^{17}, Arg^{20}, Arg^{21}, Val^{25}, Leu^{27}, and Leu^{29} in the KIM motif are important for efficient ERK2 dephosphorylation by HePTP. Interestingly, the same set of residues in PTP-SL was also found to be important for ERK2 binding in co-immunoprecipitation experiments (22), in accord with the observed increases in the K_m values for ERK2 dephosphorylation (Table IV). No significant effects were observed for the HePTP mutants Q18A, E19A, S23D, N24A, M28A, and D30A. The lack of effect on S23D is intriguing because it has been shown that Ser^{23} phosphorylation by

TABLE IV
Kinetic parameters of HePTP and its mutants with ERK2/pTpY as a substrate at pH 7 and 30 °C

HePTP	Mutation	k_{cat}	K_m	k_{cat}/K_m
		s^{-1}	μM	$M^{-1}\ s^{-1}$
Wild type	None	1.59 ± 0.11	0.61 ± 0.11	(2.61 ± 0.51) × 10^6
KIM (17–30)	ΔN 31		>2	(1.22 ± 0.02) × 10^4
	L17A	0.315 ± 0.089	4.64 ± 1.77	(6.7 ± 2.59) × 10^4
	Q18A	2.39 ± 0.11	0.50 ± 0.07	(4.78 ± 0.67) × 10^6
	E19A	2.51 ± 0.18	1.04 ± 0.16	(2.42 ± 0.37) × 10^6
	R20A		>2	(3.38 ± 0.18) × 10^5
	R21A	2.19 ± 0.25	2.32 ± 0.37	(9.44 ± 0.20) × 10^5
	R20A/R21A		>2	(3.03 ± 0.04) × 10^4
	S23D	1.33 ± 0.10	0.90 ± 0.15	(1.47 ± 0.24) × 10^6
	N24A	4.81 ± 0.38	1.41 ± 0.23	(3.40 ± 0.55) × 10^6
	V25A	1.06 ± 0.08	1.43 ± 0.21	(7.41 ± 1.09) × 10^5
	L27A		>2	(2.52 ± 0.10) × 10^5
	M28A	1.25 ± 0.05	0.55 ± 0.07	(2.26 ± 0.29) × 10^6
	L29A		>2	(3.14 ± 0.18) × 10^5
	D30A	2.60 ± 007	0.99 ± 0.06	(2.63 ± 0.16) × 10^6
α_0 (48–55)	T45E	1.69 ± 0.14	0.77 ± 0.17	(2.19 ± 0.49) × 10^6
	R47A	2.26 ± 0.07	0.41 ± 0.05	(5.51 ± 0.67) × 10^6
	E48A	1.92 ± 0.10	0.54 ± 0.09	(3.56 ± 0.59) × 10^6
	L54A	1.75 ± 0.14	0.84 ± 0.17	(2.08 ± 0.42) × 10^6
α_1-β_1 loop (85–112)	F87A	1.36 ± 0.10	0.74 ± 0.15	(1.84 ± 0.37) × 10^6
	D94A	0.89 ± 0.05	0.69 ± 0.11	(1.28 ± 0.20) × 10^6
	I95A	2.62 ± 0.21	0.67 ± 0.15	(3.91 ± 0.87) × 10^6
	Y104A	0.0291 ± 0.0030	1.42 ± 0.35	(2.04 ± 0.51) × 10^4
	K105A	2.43 ± 0.02	0.76 ± 0.18	(3.19 ± 0.76) × 10^6
	T106A	2.36 ± 0.24	1.08 ± 0.26	(2.18 ± 0.52) × 10^6
	T106D	3.26 ± 0.28	1.22 ± 0.21	(2.67 ± 0.46) × 10^6
	T106N	0.935 ± 0.045	0.61 ± 0.08	(1.53 ± 0.20) × 10^6
	T106V	1.17 ± 0.07	1.58 ± 0.22	(7.41 ± 0.11) × 10^5
	T106S	1.15 ± 0.06	0.40 ± 0.08	(2.87 ± 0.57) × 10^6
	T106L	1.09 ± 0.05	0.56 ± 0.08	(1.95 ± 0.28) × 10^6
	N110A	1.77 ± 0.31	1.66 ± 0.60	(1.07 ± 0.38) × 10^6
	P111A	1.11 ± 0.01	0.80 ± 0.18	(1.39 ± 0.31) × 10^6
WPD loop (232–243)	D236A	0.00056 ± 0.00002	< 60 nM	~9 × 10^3
	H237A	1.25 ± 0.03	0.45 ± 0.03	(2.78 ± 0.20) × 10^6
	H237F	1.09 ± 0.05	0.68 ± 0.09	(1.60 ± 0.13) × 10^6
	H237Q	1.17 ± 0.11	1.51 ± 0.30	(7.75 ± 0.30) × 10^5
	Q238G	1.47 ± 0.04	0.56 ± 0.04	(2.63 ± 0.19) × 10^6
α_5 (298–308)	Q304A	2.69 ± 0.06	0.48 ± 0.07	(5.60 ± 0.82) × 10^6
α_5-α_6 loop (309–315)	Q314A	0.67 ± 0.03	0.29 ± 0.04	(2.31 ± 0.32) × 10^6
α_6 (316–331)	Y329A	0.897 ± 0.063	0.51 ± 0.11	(1.78 ± 0.38) × 10^6

cAMP-dependent protein kinase reduces the affinity of HePTP for ERK2 (20). It is possible that an Asp at position 23 may not cause the same structural perturbations induced by phosphorylation of a Ser residue. All together, the results suggest that the KIM motif is essential for efficient ERK2 dephosphorylation by HePTP.

Role of the KIM Motif in HePTP-catalyzed ERK2 Dephosphorylation—We have established that docking interactions between the KIM motif and ERK2, likely through the CD domain, is essential to promote substrate dephosphorylation. How these docking interactions control HePTP specificity and catalysis is not understood. Do they simply tether the substrate and the enzyme, or do they precisely orient and activate them? To answer these questions and to further probe the function of KIM in HePTP catalysis, we studied several chimeric PTPs in which the NH_2-terminal segment of HePTP encompassing either the KIM sequence (residues 1–35) or the KIM sequence plus the α_0 helix (residues 1–71) is linked to the catalytic domain of PTP1B (residues 1–321). With *p*NPP as a substrate, the kinetic properties of the chimera resemble those of PTP1B (Table III), indicating that the added segment from HePTP does not interfere with the intrinsic phosphatase activity of PTP1B. Likewise, the kinetic parameters of the chimeric PTP-catalyzed hydrolysis of Tyr(P) peptides are also similar to those of PTP1B. Moreover, substitution of Asp^{48} in PTP1B with a Thr results in a 10–20-fold decrease in k_{cat}/K_m for the HePTP(1–71)/PTP1B chimera-catalyzed hydrolysis of the peptide substrates (Table III). Collectively, the results show that the presence of a KIM motif outside of PTP1B catalytic domain does not alter its activity toward *p*NPP or phosphopeptides.

Quite remarkably, the HePTP/PTP1B chimeric PTPs were more efficient enzymes (~20-fold higher in k_{cat}/K_m) than PTP1B in dephosphorylating ERK2/pTpY (Table III). No significant difference was observed between HePTP(1–35)/PTP1B and HePTP(1–71)/PTP1B, indicating that the HePTP-specific α_0 helix makes little contribution to ERK2 dephosphorylation by HePTP(1–71)/PTP1B, and the increased activity of the chimera for ERK2 is likely a result of the grafted docking interactions between the KIM motif and the CD domain. Indeed, the higher activity displayed by the chimera toward ERK2 appears to be primarily due to an increase in substrate binding affinity because the K_m values for the chimera are much lower than that of PTP1B and similar to that of HePTP. This result supports a role for the KIM motif to tether the PTP domain and ERK2, thus increasing the local substrate concentration.

However, it is clear that simple tethering is insufficient to account for the extraordinarily high activity of HePTP toward ERK2, because the k_{cat}/K_m values for the chimeric PTP-catalyzed ERK2 dephosphorylation are still ~20-fold lower than that of HePTP. This difference in catalytic efficiency is due in large part to a 10-fold lower k_{cat} of the chimeric PTPs toward ERK2 (Table III). It is possible that, in addition to increasing the "effective concentration" of the ERK2 substrate, the docking interactions between the KIM motif and the CD domain may induce an allosteric activation of the PTP domain in

HePTP but not in the context of the chimera. However, unlike MKP3, whose intrinsic phosphatase activity can be enhanced significantly upon association with ERK2 (50–52), ERK2 has no effect on the HePTP-catalyzed hydrolysis of *p*NPP and Tyr(P) peptides.[2] It is also possible that a specific set of residues unique to the MAP kinase PTPs is required for optimal ERK2 dephosphorylation. To this end, we note that none of the selected residues that are unique to the HePTP subfamily of PTPs, including Thr^{106}, seem to be essential for ERK2 dephosphorylation. We also ascertained whether Asp^{48} is responsible for the lower activity of PTP1B toward ERK2. Although Asp^{48} is important for efficient phosphopeptide hydrolysis by PTP1B, it may impede its activity toward ERK2 because a Thr residue is found at position 48 in the ERK2 specific PTPs. As shown in Table III, replacing Asp^{48} with either an Ala or a Thr did not enhance but rather decreased the k_{cat}/K_m (2–5-fold) for ERK2 dephosphorylation, in comparison with the native enzymes. Thus, in the context of PTP1B, an Asp residue is preferred over a Thr at position 48.

A more likely explanation for the robust activity of HePTP toward ERK2 is that substrate recognition by HePTP may be bipartite, requiring both the KIM/CD contact and a distinct second site interaction between the catalytic domain of HePTP and ERK2. The major function of the KIM/CD contact is to increase the "effective concentration" of ERK2, whereas a second site interaction may be essential for precise orientation and positioning of the HePTP active site with respect to $Tyr(P)^{185}$ in ERK2 for optimal dephosphorylation. Two lines of evidence suggest that the substrate-binding region in ERK2 may interact with the HePTP catalytic site. First, $Tyr(P)^{185}$ is an integral part of the $p + 1$ site for ERK2 substrate recognition (53). Second, an ERK2 specific substrate Elk1 peptide (residues 385–399, Ac-RRPRSPAKLSFQFPS-NH_2), which contains an ERK2 phosphorylation site, Ser^{389}, and a consensus F*X*FP motif that targets the ERK2 substrate-binding region (48), can completely block the HePTP-catalyzed dephosphorylation of $Tyr(P)^{185}$ in ERK2 (24). Interestingly, a similar bipartite mechanism may also be operative for the recognition of ERK2 by its cognate regulators MKP3 and MEK1 and its substrate Elk1 (48). Further studies are required to fully define the interactions between the ERK2 substrate-binding region and the HePTP catalytic site.

Conclusions—The MAP kinase ERK2 is the only known substrate for HePTP. We determined that ERK2/pTpY is a highly efficient substrate for HePTP with a k_{cat}/K_m of $2.61 \times 10^6\ M^{-1}\ s^{-1}$, which is 3 orders of magnitude higher than those for Tyr(P)-containing peptides, including an ERK2-derived phosphopeptide encompassing both $Thr(P)^{183}$ and $Tyr(P)^{185}$. To identify the structural determinants in HePTP that are important for its substrate specificity, we carried out a systematic mutational and deletion analysis of HePTP. We identified Thr^{106} in the substrate recognition loop as a key residue responsible for the reduced activity of HePTP toward Tyr(P) peptides, indicating that HePTP may have been evolved to minimize interactions with nonspecific Tyr(P) substrates. We provide evidence that the efficiency and fidelity of ERK2 dephosphorylation by HePTP is achieved by a bipartite protein-protein interaction mechanism. The docking interactions between the KIM motif and the CD site located opposite to the ERK2 activation loop promote the HePTP-catalyzed ERK2 dephosphorylation by increasing the local substrate concentration. In addition to this "tethering" effect (~20-fold increase in k_{cat}/K_m), the catalytic efficiency of HePTP toward ERK2 is further enhanced (~20-fold increase in k_{cat}/K_m) by a second site interaction involving the HePTP catalytic site and the ERK2 substrate-binding region. This interaction may be required to organize the HePTP active site with respect to $Tyr(P)^{185}$ for optimal phosphoryl transfer. Taken together, the extremely high specificity of HePTP for its physiological substrate ERK2 may be a consequence of both positive selection involving specific protein-protein interactions between HePTP and ERK2 and negative selection against nonspecific reactions with competing Tyr(P) substrates.

[2] B. Zhou and Z.-Y. Zhang, unpublished observations.

REFERENCES

1. Widmann, C., Gibson, S., Jarpe, M. B., and Johnson, G. L. (1999) *Physiol. Rev.* **79,** 143–180
2. Schaeffer, H., and Weber, M. J. (1999) *Mol. Cell. Biol.* **19,** 2435–2444
3. English, J., Pearson, G., Wilsbacher, J., Swantek, J., Karandikar, M., Xu, S., and Cobb, M. H. (1999) *Exp. Cell Res.* **253,** 255–270
4. Zhou, B., Wang, Z.-X., Zhao, Y., Brautigan, D. L., and Zhang, Z.-Y. (2002) *J. Biol. Chem.* **277,** 31818–31825
5. Yao, Z., Dolginov, Y., Hanoch, T., Yung, Y., Ridner, G., Lando, Z., Zharhary, D., and Seger, R. (2000) *FEBS Lett.* **468,** 37–42
6. Cha, H., and Shapiro, P. (2001) *J. Cell Biol.* **153,** 1355–1367
7. Zhou, B., and Zhang, Z.-Y. (2002) *J. Biol. Chem.* **277,** 13889–13899
8. Camps, M., Nichols, A., and Arkinstall, S. (2000) *FASEB J.* **14,** 6–16
9. Zhao, Y., and Zhang, Z.-Y. (2001) *J. Biol. Chem.* **276,** 32382–32391
10. Alessi, D. R., Gomez, N., Moorhead, G., Lewis, T., Keyse, S. M., and Cohen, P. (1995) *Curr. Biol.* **5,** 283–295
11. Sohaskey, M. L., and Ferrell, J. E. (1999) *Mol. Biol. Cell* **10,** 3729–3743
12. Zhan, X. L., Deschenes, R. J., and Guan, K. L. (1997) *Genes Dev.* **11,** 1690–1702
13. Karim, F. D., and Rubin, G. M. (1999) *Mol. Cell* **3,** 741–750
14. Zanke, B., Suzuki, H., Kishihara, K., Mizzen, L., Minden, M., Pawson, A., Mak, T. W. (1992) *Eur. J. Immunol.* **22,** 235–239
15. Lombroso, P. J., Murdoch, G., and Lerner, M. (1991) *Proc. Natl. Acad. Sci. U. S. A.* **88,** 7242–7246
16. Ogata, M., Sawada, M., Fujino, Y., and Hamaoka, T. (1995) *J. Biol. Chem.* **270,** 2337–2343
17. Pulido, R., Zuniga, A., and Ullrich, A. (1998) *EMBO J.* **17,** 7337–7350
18. Saxena, M., Williams, S., Gilman, J., and Mustelin, T. (1998) *J. Biol. Chem.* **273,** 15340–15344
19. Saxena, M., Williams, S., Brockdorff, J., Gilman, J., and Mustelin, T. (1999) *J. Biol. Chem.* **274,** 11693–11700
20. Saxena, M., Williams, S., Tasken, K., and Mustelin, T. (1999) *Nat. Cell Biol.* **1,** 305–311
21. Oh-hora, M., Ogata, M., Mori, Y., Adachi, M., Imai, K., Kosugi, A., and Hamaoka, T. (1999) *J. Immunol.* **163,** 1282–1288
22. Zuniga, A., Torres, J., Ubeda, J., and Pulido, R. (1999) *J. Biol. Chem.* **274,** 21900–21907
23. Pettiford, S. M., and Herbst, R. (2000) *Oncogene* **19,** 858–869
24. Wang, Z.-X., Zhou, B., Wang, Q. M., and Zhang, Z.-Y. (2002) *Biochemistry* **41,** 7849–7857
25. Zhang, Z.-Y. (2003) *Prog. Nuc. Acid Res. Mol. Biol.* **73,** 171–220
26. Puius, Y. A., Zhao, Y., Sullivan, M., Lawrence, D. S., Almo, S. C., and Zhang, Z.-Y. (1997) *Proc. Natl. Acad. Sci. U. S. A.* **94,** 13420–13425
27. Mansour, S. J., Candia, J. M., Matsuura, J. E., Manning, M. C., and Ahn, N. G. (1996) *Biochemistry* **35,** 15529–15536
28. Zhang, Z.-Y., Thieme-Sefler, A. M., Maclean, D., Roeske, R., and Dixon, J. E. (1993) *Anal. Biochem.* **211,** 7–15
29. Webb, M. R. (1992) *Proc. Natl. Acad. Sci. U. S. A.* **89,** 4884–4887
30. Szedlacsek, S. E., Aricescu, A. R., Fulga, T. A., Renault, L., and Scheidig, A. J. (2001) *J. Mol. Biol.* **311,** 557–568
31. Zhou, B., Wu, L., Shen, K., Zhang, J., Lawrence, D. S., and Zhang, Z.-Y. (2001) *J. Biol. Chem.* **276,** 6506–6515
32. Jia, Z., Barford, D., Flint, A. J., and Tonks, N. K. (1995) *Science* **268,** 1754–1758
33. Sarmiento, M., Zhao, Y., Gordon, S. J., and Zhang, Z.-Y. (1998) *J. Biol. Chem.* **273,** 26368–26374
34. Sarmiento, M., Puius, Y. A., Vetter, S. W., Keng, Y.-F., Wu, L., Zhao, Y., Lawrence, D. S., Almo, S. C., and Zhang, Z.-Y. (2000) *Biochemistry* **39,** 8171–8179
35. Keng, Y.-F., Wu, L., and Zhang, Z.-Y. (1999) *Eur. J. Biochem.* **259,** 809–814
36. Pedersen, A. K., Guo, X.-L., Møller, K. B., Peters, G. H., Andersen, H. S., Kastrup, J. S., Mortensen, S. B., Iversen, L. F., Zhang, Z.-Y., and Møller, N. P. H. (2004) *Biochem. J.* **378,** 421–433
37. Zhao, Y., Wu, L. Noh, S. J., Guan, K.-L., and Zhang, Z.-Y. (1998) *J. Biol. Chem.* **273,** 5484–5492
38. Pannifer, A. D., Flint, A. J., Tonks, N. K., and Barford, D. (1998) *J. Biol. Chem.* **273,** 10454–10462
39. Robinson, M. J., Harkins, P. C., Zhang, J., Baer, R., Haycock, J. W., Cobb, M. H., and Goldsmith, E. J. (1996) *Biochemistry* **35,** 5641–5646
40. Flint, A. J., Tiganis, T., Barford, D., and Tonks, N. K. (1997) *Proc. Natl. Acad. Sci. U. S. A.* **94,** 1680–1685
41. Zhang, Y.-L., Keng, Y.-F., Zhao, Y., Wu, L., and Zhang, Z.-Y. (1998) *J. Biol. Chem.* **273,** 12281–12287
42. Zhang, Y.-L., Yao, Z.-J., Sarmiento, M., Wu, L., Burke, T. R. Jr., and Zhang, Z.-Y. (2000) *J. Biol. Chem.* **275,** 34205–34212
43. Xie, L., Zhang, Y.-L., and Zhang, Z.-Y. (2002) *Biochemistry* **41,** 4032–4039
44. Tanoue, T., Adachi, M., Moriguchi, T., and Nishida, E. (2000) *Nat. Cell Biol.* **2,** 110–116
45. Gavin, A.-C., and Nebreda, A. R. (1999) *Curr. Biol.* **9,** 281–284

46. Smith, J. A., Poteet-Smith, C. E. Malarkey, K., and Sturgill, T. W. (1999) *J. Biol. Chem.* **274,** 2893–2898
47. Nichols, A., Camps, M., Gillieron, C., Chabert, C., Brunet, A., Wilsbacher, J., Cobb, M., Pouyssegur, J., Shaw, J. P., and Arkinstall, S. (2000) *J. Biol. Chem.* **275,** 24613–24621
48. Zhang, J., Zhou, B., Zheng, C.-F., and Zhang, Z.-Y. (2003) *J. Biol. Chem.* **278,** 29901–29912
49. Bardwell, A. J., Abdollahi, M., and Bardwell, L. (2003) *Biochem. J.* **370,** 1077–1085
50. Camps, M., Nichols, A., Gillieron, C., Antonsson, B., Muda, M., Chabert, C., Boschert, U., and Arkinstall, S. (1998) *Science* **280,** 1262–1265
51. Zhou, B., and Zhang, Z.-Y. (1999) *J. Biol. Chem.* **274,** 35526–35534
52. Fjeld, C. C., Rice, A. E., Kim, Y., Gee, K. R., and Denu, J. M. (2000) *J. Biol. Chem.* **275,** 6749–6757
53. Canagarajah, B. J., Khokhlatchev, A., Cobb, M. H., and Goldsmith, E. J. (1997) *Cell* **90,** 859–869

Molecular Determinants of Substrate Recognition in Hematopoietic Protein-tyrosine Phosphatase

Zhonghui Huang, Bo Zhou and Zhong-Yin Zhang

J. Biol. Chem. 2004, 279:52150-52159.
doi: 10.1074/jbc.M407820200 originally published online October 4, 2004
